

As a minor note, we have considered for oxygen gas values one-half the stopping cross section of molecular O_2 gas.⁸ This allows the possibility that it may be O_2 which violates Bragg's Rule by twice our correction factor, and that the solids of Table I may be in accord with oxygen stopping cross sections if it could be measured in the atomic state. This appears improbable because of the generalized gas-solid evaluation shown in Fig. 2.

In summary, we have found that the energy loss of He^+ in gases appears systematically higher than in solids when the He^+ velocity approaches electron orbital velocities. We have also estimated the energy loss of He^+ in oxygen in solid compounds by backscattering yield measurements and find these oxygen values differ from oxygen gas values in agreement with the general solid-gas differences. We find that for one solid compound, nitrogen energy-loss values differ from nitrogen gas values also as predicted. Numerical values of the solid-state stopping cross sections for N and O will be published elsewhere.¹⁷

*Permanent address: Electrical Engineering Dept., California Institute of Technology, Pasadena, Calif. 91125.

¹Over 200 recent references to material analysis using nuclear reactions, nuclear backscattering, ion-induced x rays, etc., are found in *Ion Beam Surface Layer Analysis*, edited by J. W.

Mayer and J. F. Ziegler (Elsevier Publishing Co., Lausanne, 1974).

²See, for example, W. Whaling, *Handbuch der Physik* (Springer, Berlin, 1958), Vol. 34, p. 193.

³See, for example, J. Lindhard and M. Scharff, *Phys. Rev.* **124**, 128 (1961), or A. Teplova, V. S. Nikolaev, I. S. Dmitriev, and L. N. Fateeva, *Sov. Phys.-JETP* **15**, 31 (1962).

⁴W. K. Chu, V. L. Moruzzi, and J. F. Ziegler (*J. Appl. Phys.* **46**, 2817 (1975).

⁵W. F. G. Swann, *J. Franklin Inst.* **226**, 598 (1938).

⁶E. Fermi, *Phys. Rev.* **57**, 485 (1940).

⁷C. A. Sautter and E. J. Zimmerman, *Phys. Rev.* **140**, A490 (1965).

⁸P. D. Bourland, W. K. Chu, and D. Powers, *Phys. Rev. B* **3**, 3625 (1971); P. D. Bourland and D. Powers, *Phys. Rev. B* **3**, 3635 (1971).

⁹D. Powers, W. K. Chu, R. J. Robinson, and A. S. Lodhi, *Phys. Rev. A* **6**, 1425 (1972).

¹⁰D. Powers, A. S. Lodhi, W. K. Lin, and W. L. Cox, Jr., *Thin Solid Films* **19**, 205 (1973).

¹¹A. S. Lodhi and D. Powers, *Phys. Rev. A* **10**, 2131 (1974).

¹²W. H. Bragg and R. Kleeman, *Philos. Mag.* **10**, S318 (1905).

¹³J. F. Ziegler and W. K. Chu, *At. Data Nucl. Data Tables* **13**, 463 (1974).

¹⁴J. S.-Y. Feng, W. K. Chu, and M.-A. Nicolet, *Phys. Rev. B* **9**, 3881 (1974).

¹⁵O. Meyer, G. Linker, and B. Kraeft, *Thin Solid Films* **19**, 217 (1973).

¹⁶Electrochemical Soc. Ext. Abstr. **3**, (1966). Over twenty papers discuss the difficulties of obtaining stoichiometric thin-film nitrides.

¹⁷J. F. Ziegler and W. K. Chu, *J. Appl. Phys.* (to be published).

Mixed metal vapor phase matching for third-harmonic generation*

D. M. Bloom, J. F. Young, and S. E. Harris

Microwave Laboratory, Stanford University, Stanford, California 94305
(Received 10 June 1975)

Phase matching for frequency tripling of $1.06 \mu\text{m}$ is demonstrated in a homogeneous mixture of sodium and magnesium vapor. The ratio of Mg to Na vapor pressures required for phase matching is 2:1. This ratio is about 1/75 of that required to phase match Na with Xe.

PACS numbers: 42.65.F

One of the limitations on efficient third-harmonic generation in alkali metal vapors is the high buffer gas pressure which is required for phase matching.¹ In this Letter, we report phase matching of an alkali metal vapor by homogeneous mixing with Mg vapor. Since the resonance line of Mg (2852 \AA) is much closer to the visible spectrum than are those of the inert gases, the necessary ratio of Mg vapor to alkali metal vapor is much smaller than that for phase matching with an inert gas. This lower phase-matching ratio may ultimately allow higher pressures of the alkali metal vapor and may, thus, result in higher conversion efficiencies at a given level of input power. The absence of a high-pressure phase-matching gas also reduces the impor-

tance of three-body processes such as dimer and excimer formation.

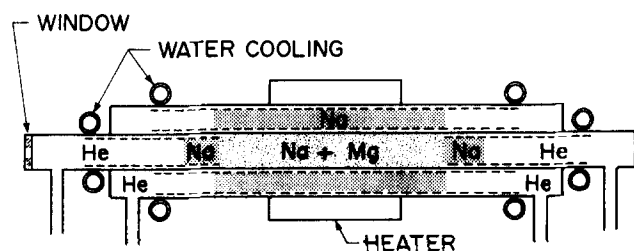


FIG. 1. Schematic of two-metal heat-pipe oven.

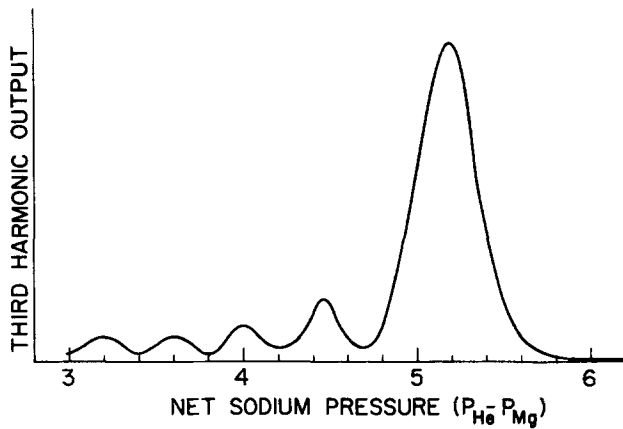


FIG. 2. Relative output power vs sodium pressure; magnesium pressure, 11 Torr; laser confocal parameter, 33 cm.

To obtain a uniform mixture of Na and Mg vapor, we constructed a two-metal heat-pipe oven of the type described by Vidal and Hessel.² The cell was similar to the Na-Xe concentric heat-pipe oven which we described previously,³ except that the wick inside the inner tube was removed to allow a 50-cm wickless region in the cell center. As shown in Fig. 1, the outer heat pipe contained pure Na and functioned to provide a constant-temperature environment for the inner pipe. Since the Mg occupies the wickless region of the inner pipe, its partial pressure is determined by the surrounding temperature which is, in turn, determined by the He pressure in the outer pipe. The Na in the end (wicked) sections of the inner pipe operates in a heat-pipe mode with a partial pressure equal to that of the inner-pipe He buffer gas. The partial pressure of the Na in the central (wickless) region of the inner pipe is such that the sum of its partial pressure and the partial pressure of the Mg is equal to the total pressure of the He buffer gas. Thus, by independently varying the partial pressures of He in the inner and outer pipes, the absolute concentration of Na and the ratio of Mg to Na may be varied.

Since the vapor pressure of Mg at its melting point is about 3 Torr, it has a tendency to condense as a solid on the wick. This leads to quite rapid depletion of the Mg in the central portion of the cell. At operating pressures of 5–10 Torr the cell could be operated for several hours before additional Mg need be added. However, at total pressures above 20 Torr the Mg was depleted even before the oven could be fully heated. In order to overcome this problem, a loader was constructed so that the Mg could be added to the cell after the cell was heated. This technique allowed operation of the cell at pressures above 20 Torr, but operating times were limited to about $\frac{1}{2}$ h. Furthermore, due to the rapid loss of Mg, it was difficult to optimize the phase-matching ratio.

The laser and data collection electronics were the same as described in Ref. 3. Phase-matching data were obtained by fixing the Mg pressure and varying the Na pressure by adjusting the He pressure in the inner

chamber. A typical phase-matching curve is shown in Fig. 2. From these measurements, a phase-matching ratio for Mg:Na of 2:1 was obtained for the $1.06 \mu\text{m} \rightarrow 3547 \text{ \AA}$ conversion process. This may be compared with a ratio of 152:1 for Xe to Na.

Energy conversion efficiency versus incident power density is shown in Fig. 3. The highest conversion efficiency which we could obtain in these experiments was 3.75%. This occurred at a Na density of 1.3×10^{17} atoms/cm³. Attempts to further increase the Na pressure resulted in broader phase-matching curves, indicating poor homogeneity. As indicated above, we believe that this is due to the rapid depletion of Mg from the cell center.

Though the maximum conversion efficiency which we obtained in this experiment (3.75%) is not as great as that which we have obtained by phase matching of Rb with Xe (10%),³ we believe that metal-metal matching of the type described here has great promise. If the metal mixing and homogeneity problems can be solved, this technique may allow tripling cells to be operated at a much higher density of the nonlinear specie. At a given power density, and cell length, conversion efficiency increases as the square of this density. One possible solution to the mixing and homogeneity problems encountered here is the rotating heat pipe described by Hessel and Lucatorto.⁴

The authors gratefully acknowledge helpful discussions with M. M. Hessel and T. B. Lucatorto.

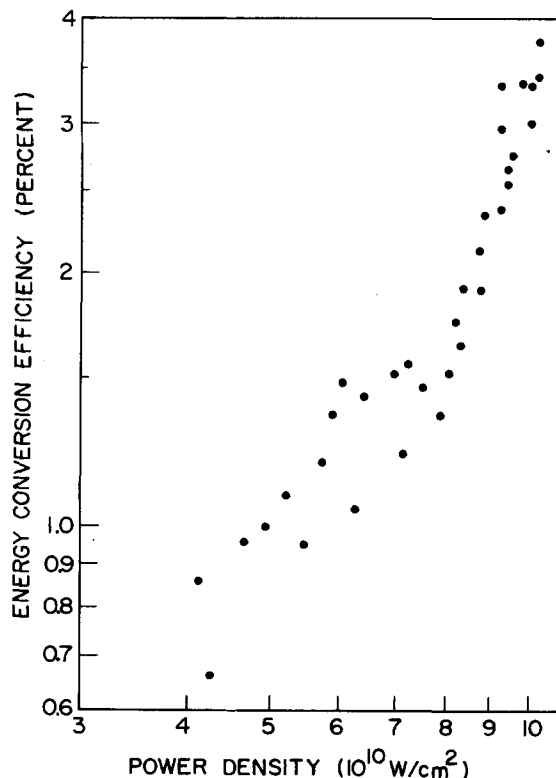


FIG. 3. Conversion efficiency vs $1.06\text{-}\mu\text{m}$ power density. Sodium atom density, $1.3 \times 10^{17} \text{ cm}^{-3}$; laser confocal parameter, 33 cm; zone length, 50 cm.

* This research was supported by the University of California and the Atomic Energy Commission and the National Aeronautics and Space Administration under Contract No. NGL 05-020-103.

¹R. B. Miles and S. E. Harris, IEEE J. Quantum Electron. QE-9, 470 (1973).

²C. R. Vidal and M. M. Hessel, J. Appl. Phys. 43, 2776 (1972).

³D. M. Bloom, G. W. Bekkers, J. F. Young, and S. E. Harris, Appl. Phys. Lett. 26, 687 (1975).

⁴M. M. Hessel and T. B. Lucatorto, Rev. Sci. Instrum. 44, 561 (1972).

A new luminescence line due to nitrogen implanted into $\text{Al}_x\text{Ga}_{1-x}\text{As}$ ($x = 0.37$)

Shun-ichi Gonda and Yunosuke Makita

Electrotechnical Laboratory, Tanashi, Tokyo, Japan
(Received 25 April 1975; in final form 10 July 1975)

Optical behavior of isoelectronic impurities in $\text{Al}_x\text{Ga}_{1-x}\text{As}$ ($x = 0.37$) is investigated. Photoluminescence of the samples implanted with N was measured at 2°K. A new luminescence line is observed at an energy which is 90 meV below the edge emission peak. The integrated intensity of the N-implanted sample is about five times larger than that of an unimplanted and annealed sample. This is thought to be due to the bound states produced by the N atoms which replace the As atoms.

PACS numbers: 78.60.D

Isoelectronic impurities such as N atoms are known to be efficient radiation recombination centers in GaP, $\text{GaAs}_{1-x}\text{P}_x$, and $\text{In}_x\text{Ga}_{1-x}\text{P}$ ¹ and are often used in LED and optically pumped lasers.² As far as we know, no report has been presented concerning the formation of isoelectronic traps in AlAs-GaAs mixed crystals. In the case of AlAs, Lorenz *et al.* suggested the presence of isoelectronic traps from absorption measurements.³ Nitrogen in GaAs does not form isoelectronic traps. How do isoelectronic impurities behave optical in AlAs-GaAs mixed crystals? This letter presents an experimental investigation of the photoluminescence of isoelectronic impurities in $\text{Al}_x\text{Ga}_{1-x}\text{As}$ ($x = 0.37$). There are several prospective atoms which are isoelectronic in $\text{Al}_x\text{Ga}_{1-x}\text{As}$. As a first step, nitrogen atoms in direct-gap $\text{Al}_x\text{Ga}_{1-x}\text{As}$ ($x = 0.37$) were examined. As a method of doping, ion implantation was used in order to obtain a uniform and spatially well-controlled distribution of impurity atoms. The results of photoluminescence (PL) measurements for $\text{Al}_x\text{Ga}_{1-x}\text{As}$ implanted with N will be given and discussed.

The $\text{Al}_x\text{Ga}_{1-x}\text{As}$ ($x = 0.37$) layers, typically 10 μm thick, were grown by LPE on the (100) surface of Si-doped *n*-GaAs. LPE layers were not intentionally doped. The *x* value is determined from the PL spectra using the empirical formula of Onton *et al.*⁴ Prior to implantation, no special treatment was given to the wafer surface. Ion implantation was performed at 350 °C, at energies between 50 and 220 keV, using a mass-separated beam of N⁺ or Ne⁺ ions. Neon ions, which were surmised to be nonluminescent centers in the material, were introduced in order to investigate the effect of radiation damages. In this situation a theoretical calculation predicts that the concentration profile of implanted atoms has a plateau of about $1 \times 10^{18} \text{ cm}^{-3}$ in the range between 0.1 and 0.45 μm below the surface. The wafers were covered with SiO_x by Ar⁺ sputtering and

annealed in vacuum up to 825 °C for 30 min. Photoluminescence studies were made at 2 °K. The photoluminescence was excited with the 514.5-nm line from a cw Ar⁺ laser or the 585.0-nm line from a pulsed dye laser. The spectra were measured with a Spex model 1704

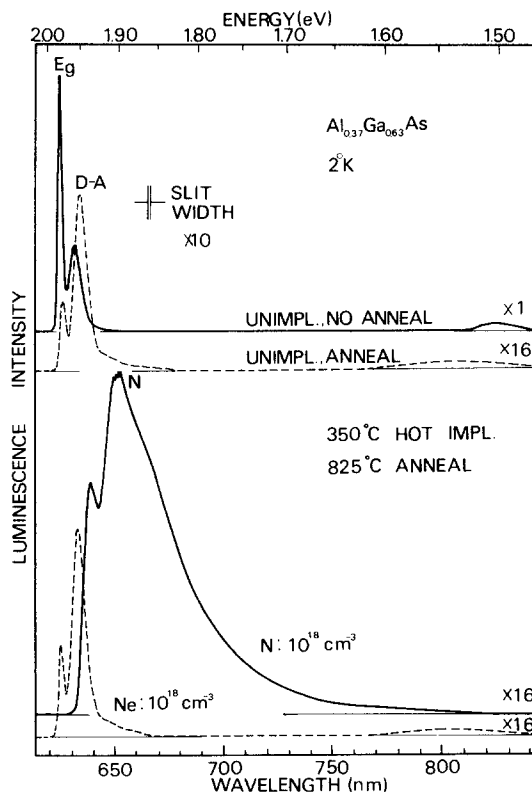


FIG. 1. Photoluminescence spectra at 2°K for $\text{Al}_x\text{Ga}_{1-x}\text{As}$ unimplanted and not annealed, unimplanted and annealed at 825 °C for 30 min, implanted with N and annealed (N), and implanted with Ne and annealed (Ne).